ELSEVIER

Journal of Power Sources 80 (1999) 46–52

JOURNAL OF POWER SOURCES

In-plane compression porometry of battery separators

Akshaya K. Jena *, Krishna M. Gupta

Porous Materials, 83 Brown Road, Ithaca, NY 14850, USA

Received 1 February 1999; accepted 1 February 1999

Abstract

We have designed equipment that measures, by means of capillary flow porometry, the pore structure of sheet materials. The equipment measures the influence of superimposed compressive stress on pore structure as well. The bubble point pressure, mean flow pressure, and flow distribution of a battery separator have been measured, and the influence of compressive stresses on these parameters have been observed. Our results demonstrate that the pore structure for in-plane flow is considerably different from that for flow in the perpendicular direction, and the effect of superimposed compressive stress is appreciable. © 1999 Elsevier Science S.A. All rights reserved.

Keywords: Capillary flow porometry; Pore structure; Battery separators

1. Introduction

Battery separators are sheets of fibrous material. The porous structure of the material allows the flow of electrolytes in batteries. The performance of separators depends upon the relative magnitudes of their permeability in different directions. Permeability is governed by the pore structures. The pore structures are normally characterized by measuring the bubble point pore diameter, the mean flow pore diameter and the flow distribution in a capillary flow porometer. In a battery separator, the pore structure in the direction parallel to the thickness of the sheet (through-plane) is different from that in the direction parallel to the plane of the sheet (in-plane). Consequently, evaluations of pore characteristics in the two directions differ.

Battery separators are subject to compressive stress during application. Such stress can appreciably modify the pore structure and permeability of the material. However, the pore structure of battery separators are commonly measured using techniques that determine the unstressed through-plane pore structure and ignore the in-plane pore structure, as well as the effects of compression applied to both the through-plane and in-plane pore structures. Thus, we set out to characterize the in-plane pore structure, and to determine the effects of compression on the in-plane and through-plane pore structures, of battery separators.

2. Materials and methods

For this study we used the completely automated PMI Capillary Flow Porometer [1,2], which is capable of giving reproducible results [3]. To determine the pore characteristics of a material using a capillary flow porometer, we soak a sample of material in a liquid which fills the pores of the material, and then apply gas pressure on one side of the sample which forces the liquid out of the pores. At low gas pressures the flow rate is zero. Flow starts at a low pressure, which is sufficient to clear some of the pores. As the pressure increases more pores get emptied, and the flow rate increases. The flow rate is determined as a function of pressure and is used to calculate the desired pore characteristics.

The sample chamber of the instrument was modified to measure the in-plane pore structure under compression. Fig. 1 illustrates the important features of the chamber. An outline of the arrangement of different components for through-plane measurement is shown in Fig. 1(a) and that for in-plane measurement in Fig. 1(b). For through-plane studies, the sample rests on the o-ring at the bottom of the sample chamber. The insert is placed on the o-ring on top of the sample. The cap is placed on the sample chamber and the insert. In this arrangement, escape of gas between the insert and the sample chamber is prevented by the o-rings placed between these two components; gas flows through the sample parallel to its thickness and escapes to the atmosphere through the central holes in the insert and

* Corresponding author

PII: S0378-7753(99)00163-9

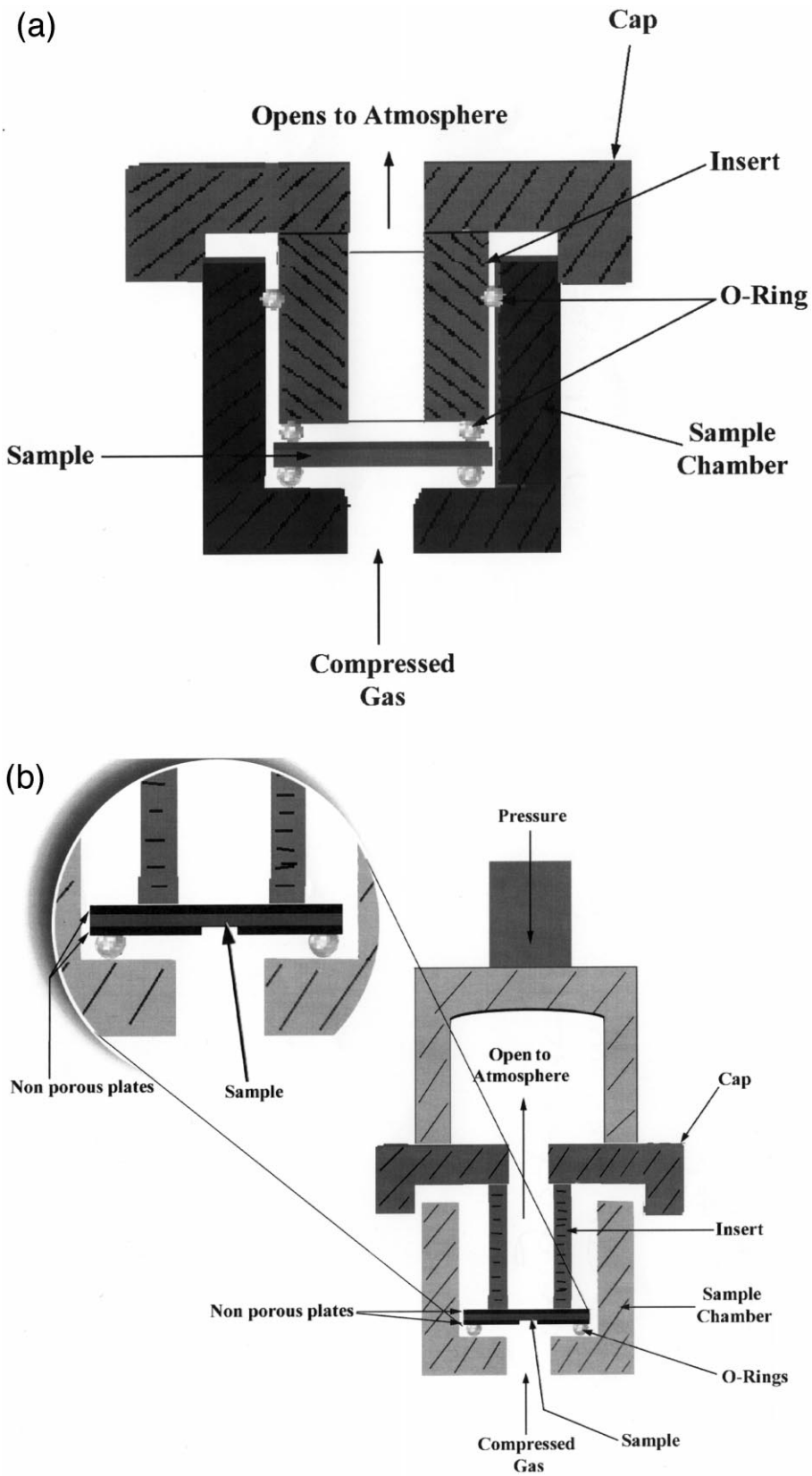

Fig. 1. Sample chamber. (a) Through-plane. (b) In-plane.

the cap. For in-plane studies (Fig. 1(b)), the sample is placed between two nonporous plates. The bottom plate contains a central hole for the gas to access the bottom surface of the sample. Compressed gas passes through the central opening in the bottom plate, flows parallel to the planar surface of the sample, and escapes to the atmosphere between the sample chamber and the insert. The liquid film present between the sample and the nonporous plates is adequate to prevent leakage between the sample and the nonporous plates. The desired amount of compressive stress is applied to the top. The sample diameter is kept slightly larger than the diameter of the nonporous plate so that the wetting liquid may be added to the sample prior to subsequent testing without disturbing the sample.

We investigated the battery separator Hovosorb manufactured by Hollingsworth and Vose. A low surface tension wetting liquid, Porewick™ was used to fill the pores in the sample. The flow rate as a function of pressure was measured for both a wet sample and a dry sample. Data gathered from this experiment was used to calculate other parameters of the pore structure.

3. Results and discussion

3.1. Bubble point pressure

Bubble point pressure is the minimum amount of pressure required for flow to pass through a wet sample. Measurements of bubble point pressure in the through-plane and in-plane directions are listed in Table 1. These two values are considerably different from each other.

In our experiments, the sample is soaked in a liquid that fills the empty pores in the sample spontaneously, and gas is used to force the liquid out of the pores by gradually increasing the pressure of the gas. Filling of the pores involves creation of solid/liquid interfaces in place of solid/gas interfaces. If the solid/gas interfacial free energy is higher than the solid/liquid interfacial free energy, the process of filling the pores with liquid will decrease the free energy of the system and make the process spontaneous. Alternately, when the gas displaces the liquid inside the pore, the solid/gas interface is created in place of the solid/liquid interface, and the free energy of the system increases. In order to displace the liquid inside the pore, the gas does work on the system to compensate for the increase in the interfacial free energy [4]. The work done by the gas is represented by $p\mathrm{d}V$, where p is the gas pressure and $\mathrm{d}V$ is the infinitesimal increase in volume of the gas inside the pore. The work done by the gas must be equal to the increase in the interfacial free energy. The increase in the interfacial free energy is determined by the interfacial free energy per unit area and the interfacial area, which is related to the void structure of the material.

The interconnected voids create the path for gas flow in the sample. Shapes of the voids depend on how the material was manufactured. The battery separator Hovosorb is fibrous. The structure of the in-plane of Hovosorb is shown in the scanning electron micrograph (Fig. 2). Such a structure has lots of unfilled space (openings), which are crisscrossed and penetrated by small and large fibres in a seemingly random manner. The surface area of this material is the outer surfaces of the fibres. When gas displaces liquid in an opening in such a structure, the extent of the fibre (solid)/liquid interfacial area that is replaced by the fibre (solid)/gas interfacial area is determined by the number of fibres that surround the opening and intercept the space in the opening.

Table 1
Bubble point and mean flow pressure and diameters

	Bubble point		Mean flow	
	Pressure (kPa)	Diameter (μm)	Pressure (kPa)	Diameter (μm)
In-plane	3.482	13.148	10.258	4.463
Through-plane	2.751	16.641	5.186	8.827

Fig. 3 illustrates the displacement of the liquid in an opening of a fibrous material. It is clear that the displacement results in increases of the solid/gas and the liquid/gas interfacial areas. Consider a small displacement of the gas inside an opening, such that the increase in the volume of the gas is $\mathrm{d}V$, and increases in the solid/gas and the liquid/gas surface areas are $\mathrm{d}S_{s/g}$ and $\mathrm{d}S_{l/g}$, respectively. The following formula equates the work done by the gas to the increase in interfacial free energy:

$$p\,\mathrm{d}V = (\gamma_{s/g} - \gamma_{s/l})\,\mathrm{d}S_{s/g} + \gamma_{l/g}\mathrm{d}S_{l/g} \quad (1)$$

where $\gamma_{l/g}$ = liquid/gas interfacial free energy, $\gamma_{s/g}$ = solid/gas interfacial free energy, and $\gamma_{s/l}$ = solid/liquid interfacial free energy. Eq. (1) may be written as:

$$p = \gamma_{l/g}\,\beta(\mathrm{d}S_{s/g}/\mathrm{d}V)[1 + (f/\beta)] \quad (2)$$

where,

$$\beta = (\gamma_{s/g} - \gamma_{s/l})/\gamma_{l/g}$$

$$f = (\mathrm{d}S_{l/g}/\mathrm{d}S_{s/g})$$

Equilibrium between the three interfacial free energies suggests that [5]:

$$\cos\theta = (\gamma_{s/g} - \gamma_{s/l})/\gamma_{l/g} \quad (3)$$

where θ is the contact angle, $\beta = \cos\theta$, and β has a value of ≤ 1. However, if the interfacial free energies are such that equilibrium is not possible, β would be < 1 [3]. It has been shown that when wetting liquids with small values of interfacial free energies are used, β may be taken as 1 [3].

The value of f in Eq. (2) is not known. However, the magnitude of f in Hovosorb may be estimated. By taking approximate values of the maximum opening diameter, fibre diameter, and fibre density from Fig. 2, the magni-

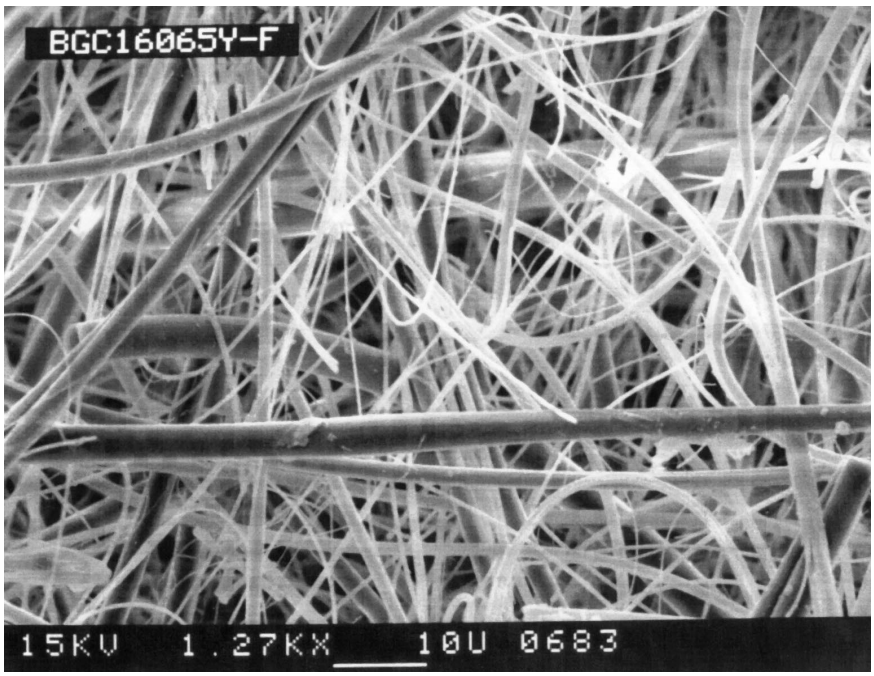

Fig. 2. Scanning electron micrograph of Hovosorb.

tude of f is found to be much less than one. Under these conditions Eq. (2) reduces to:

$$p = \gamma_{l/g}(dS_{s/g}/dV) \quad (4)$$

For a specific combination of liquid, gas, and sample material, the interfacial free energies are fixed. Hence, the first term on the right hand side of Eq. (4) is a constant. However, the second term, $(dS_{s/g}/dV)$, is a function of the path of the gas; but gas flows through many paths. The pressure necessary for the gas to flow along a given path is determined by the highest value of $(dS_{s/g}/dV)$ along that path. The bubble point pressure is the pressure required to clear the path through which the gas first escapes the sample. Hence, the bubble point pressure is determined by the value of $(dS_{s/g}/dV)$, that is, the lowest amongst the highest values for all paths.

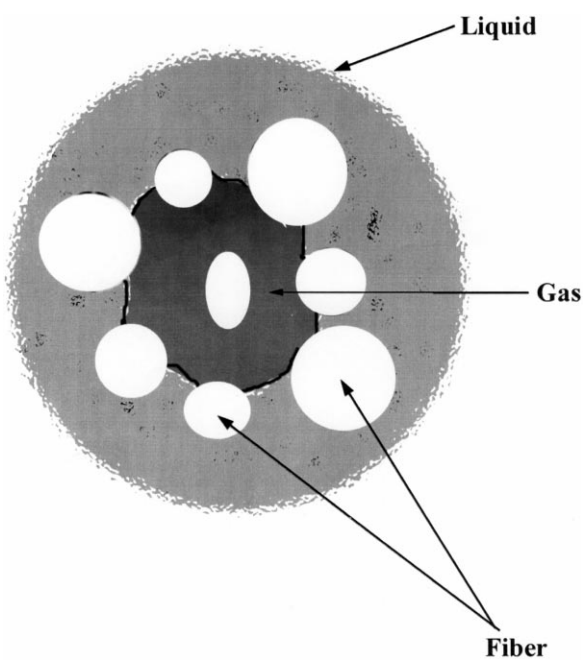

Fig. 3. Sketch of a gas-containing opening in fibrous structure.

It is convenient to visualize pores in terms of diameters rather than ratios. For a cylinder of diameter D:

$$(dS_{s/g}/dV) = 4/D \quad (5)$$

If we represent a pore at any location along its length by the diameter, D, of a cylinder, such that $(dS_{s/g}/dV)$ of the pore is the same as that of the cylinder, Eq. (4) becomes:

$$D = (4\gamma_{l/g})/P \quad (6)$$

The bubble point pore diameter calculated using Eq. (6) is listed in Table 1. If the fibres in the Hovosorb were randomly oriented, the in-plane and the through-plane bubble point pressures would not differ appreciably. However, in close examination Fig. 2 shows that the orientation of the fibres is not completely random. The long dimensions of the fibres are mostly parallel to the surface of the sheet. Therefore, the openings parallel to the surface are different from those in the direction of thickness. Consequently, the bubble point pressures are appreciably different (Table 1).

3.2. Mean flow pressure

Mean flow pressure is the pressure at which the amount of flow that passes through a wet sample is one-half of the

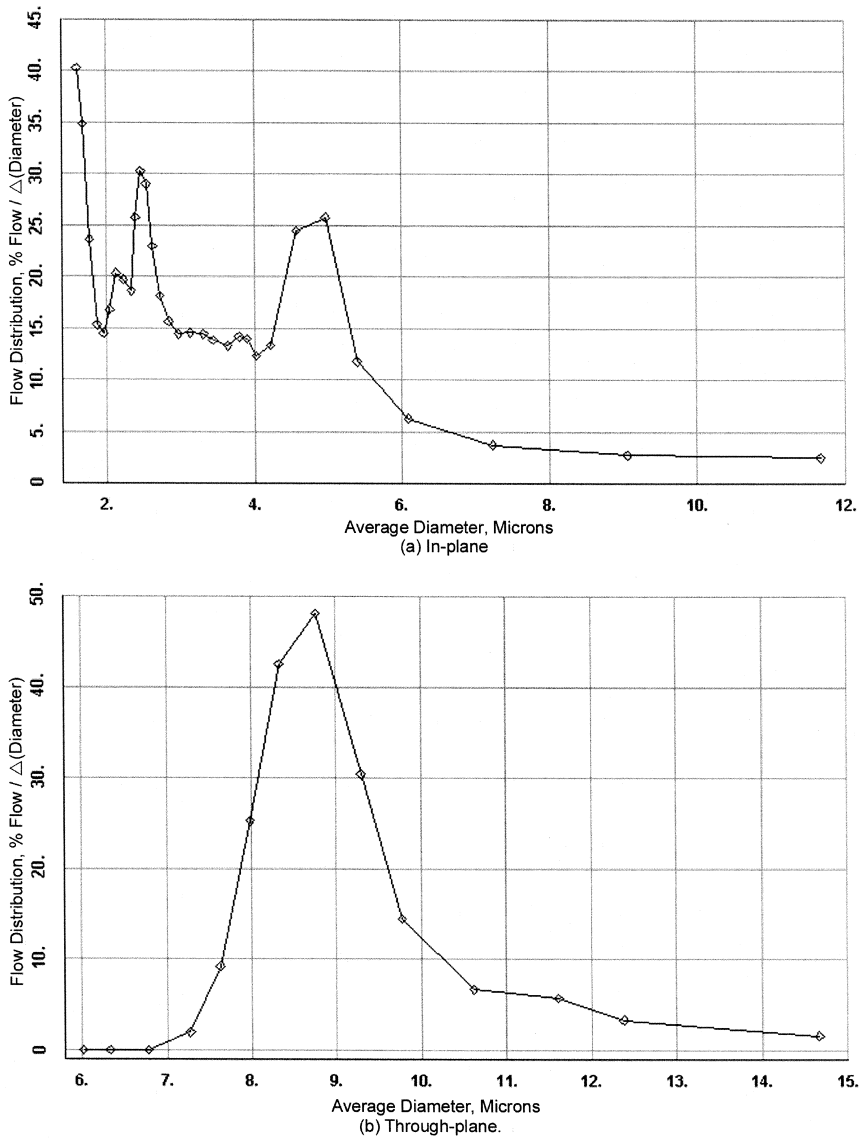

Fig. 4. Flow distribution. (a) In-plane. (b) Through-plane.

flow that passes through a dry sample. The mean flow pressures and the mean flow pore diameters for the through-plane and the in-plane directions are listed in Table 1. These two sets of values are considerably different from one another.

3.3. Flow rate distribution

The percentage flow of gas through pores having diameters within narrow specified ranges was calculated from the experimental data. These results are presented in Fig. 4 as plots of [% flow/ΔD] against D. Such plots are often referred to as pore size distributions. They essentially give the amount of flow through pores of a given diameter. The distribution of flow over pores of various sizes for through-plane and in-plane flow is considerably different in the two directions.

3.4. Anisotropy of in-plane flow

A number of experiments were interrupted before the in-plane bubble point pressure was detected, and the sam-

Table 2
Effect of compression on bubble point pore diameter and mean flow pore diameter during in-plane flow

Stress (kPa)	Pore diameter (μm)	
	Bubble point	Mean flow
0	13.1	4.46
34.5	11.4	3.18
103	9.71	3.42
172	8.32	2.36
207	7.86	2.29
276	7.58	2.27
379	6.53	1.90

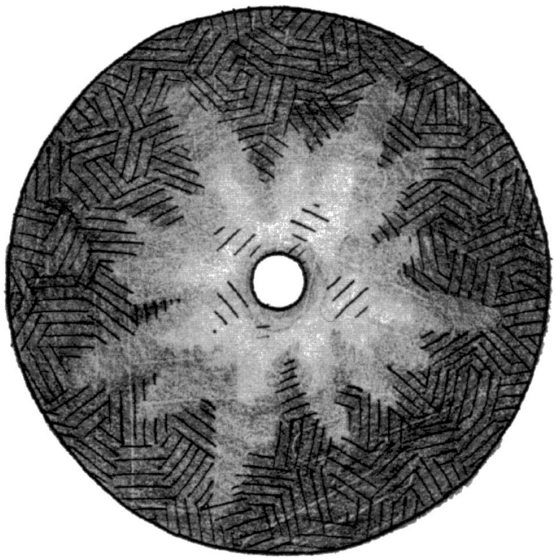

Fig. 5. In-plane flow pattern.

ple was removed for examination. The central part of the sample that had been penetrated by the gas was dry, the outer part was wet, and the part in between was partially wet. These three regions could be easily observed in the sample. One such sample is shown in Fig. 5. A material possessing cylindrically symmetrical pore distribution must show concentric circular regions. The penetration of gas appears to be more abundant in some of the radial directions than in others (Fig. 5). This demonstrated a more asymmetrical pattern in their radial directions.

We surmised that because gas has the tendency to move preferentially along openings in the plane that have less number of fibres intercepting the opening, and due to the statistical distribution of the fibres, the regions surrounding these openings have more fibres, and hence, have reduced gas flow. This is seen in Fig. 5. Since the fibres are randomly distributed in the plane, the preferential gas flow directions for in-plane flow are also randomly distributed.

3.5. Influence of compressive stress on in-plane flow

The bubble point pore diameters and the mean flow pore diameters determined under compressive stresses during in-plane flow are listed in Table 2. Compressive stresses have the tendency to reduce the pore diameter. This is demonstrated by the data in Table 2.

The effect of compression on flow distribution is demonstrated in Fig. 6, which gives the flow distributions in the sample under 276 kPa compressive stress. The entire distribution curve has moved to lower pore sizes.

The results displayed above show that the pore diameters tend to decrease, at a decreasing rate, with an increase in the compressive stress. Application of stress tends to compress the pores. If the pore is considered to have a square cross section of side, δ, application of stress will make the cross-section rectangular with its long side, δ_1, perpendicular to the stress axis and the short side, δ_2, parallel to the stress axis. δ_2 is given by $\delta(1-\varepsilon)$ where ε is the strain (thickness change/thickness) in the sample. Assuming that upon application of stress the perimeter of the opening remains essentially the same while its cross-sectional area changes, $\delta_1 = \delta(1+\varepsilon)$. Hence:

$$\left(\mathrm{d}S_{s/g}/\mathrm{d}V\right)_{\sigma=0} = 4/\delta \tag{7}$$

$$\left(\mathrm{d}S_{s/g}/\mathrm{d}V\right)\sigma = \left[(2/\delta_1) + (2/\delta_2)\right] = 4/\left(\delta\left[1-\varepsilon^2\right]\right) \tag{8}$$

From Eqs. (4), (7) and (8):

$$p_{\sigma=0} = 4\gamma_{l/g}/\delta \tag{9}$$

$$p_{\sigma} = 4\gamma_{l/g}/\delta(1-\varepsilon^2) \tag{10}$$

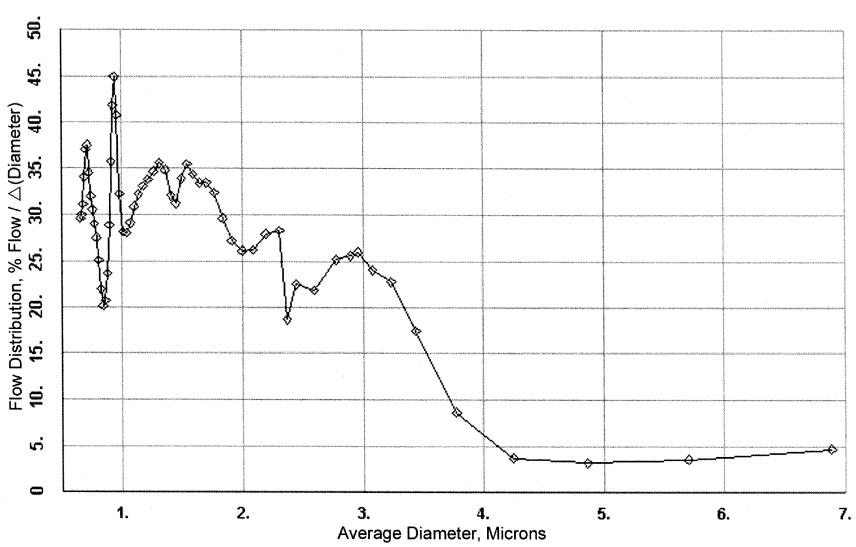

Fig. 6. In-plane flow distribution under 276 kPa compressive stress.

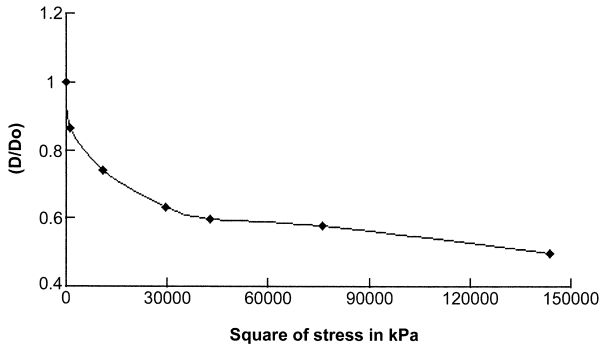

Fig. 7. Variation of the ratio of the bubble point diameters measured under stress and under no stress, with square of stress.

The measured pore diameters, D_0 at no stress, and D at stress σ, are after Eq. (6):

$$D_0 = 4\gamma_{l/g}/p_{\sigma=0} \quad (11)$$

$$D = 4\gamma_{l/g}/p_{\sigma} \quad (12)$$

From Eqs. (9)–(12):

$$D/D_0 = 1 - \varepsilon^2 \quad (13)$$

As the stress is applied, the space within the pores is squeezed out rapidly in the initial stages. However, in the later stages the strain is likely to be proportional to stress. Let $\varepsilon = c\sigma$, where c is a constant. Hence:

$$D/D_0 = 1 - c^2\sigma^2 \quad (14)$$

Fig. 7 shows the variation of (D/D_0) with σ^2. After the initial transient period, the pore diameter changes in the manner predicted by Eq. (14). Thus, the simple model presented here explains the dependence of pore diameter on applied compressive stress.

4. Conclusions

(1) Equipment has been fabricated to measure pore structure of a sheet material parallel to the plane of the sheet (in-plane) by capillary flow porometry. The equipment can also measure the pore structure for in-plane flow as a function of applied compressive stress.

(2) In-plane and through-plane (parallel to the thickness) bubble point pressures, mean flow pressures and flow distributions have been measured. These properties are considerably different for both directions.

(3) In-plane bubble point pressure, mean flow pressure and flow distribution have been measured as functions of applied compressive stress. The effect of compressive stress is appreciable.

(4) Analysis of the data shows that the results are consistent with the fibrous structure of the battery separator. The dependence of pore diameter on compressive stress has been satisfactorily explained in terms of the model.

References

[1] Ron V. Webber, Filtration News, Jan/Feb (1994) 52.
[2] C. Rebecca Stillwell, Proceedings of the 7th World Filtration Congress, Budapest, Hungary, May, 1994.
[3] Vibhor Gupta, A.K. Jena, Proceedings of the 12th Annual AFS Technical Conference, April, 1999 (Accepted).
[4] K. Denbigh, The Principles of Chemical Equilibrium, Cambridge Univ. Press, 1968.
[5] A.W. Adamson, Physical Chemistry of Surfaces, Interscience, 1967.